Multi-Heme Self-Assembly in Phospholipid Vesicles

Joydeep Lahiri, Gwendolyn D. Fate, Solomon B. Ungashe, and John T. Groves*

Contribution from the Department of Chemistry, Princeton University, Princeton, New Jersey 08544

Received September 7, 1995[⊗]

Abstract: The use of weak, intermolecular forces to orchestrate the contruction of multicomponent systems in membranes has significant implications in diverse areas of chemistry, biology, and medicine. We describe here the construction and characterization of multi-heme molecular ensembles in phospholipid vesicles. A trianionic zinc porphyrin was designed to bind cytochrome *c* at the membrane surface, while being anchored to a membrane spanning manganese porphyrin in the membrane interior via a terminal imidazole. The structure of the construct was probed by fluorescence and UV spectroscopy. Cytochrome *c* formed a stoichiometric 1:1 complex with the anionic porphyrin with a high binding constant ($K_a \approx 5 \times 10^6$ M^{-1}). The ligation of the imidazole to the manganese porphyrin was confirmed by UV spectral changes. Large differences in the fluorescence quenching of Zn porphyrins with and without the terminal imidazole were observed upon their insertion into vesicles containing the Mn porphyrin. These spectroscopic observations were consistent with the formation of a ligated, ternary system consisting of the Mn(II) porphyrin, the imidazole-tailed zinc porphyrin acting as a bridge, and the surface associated cytochrome *c*. The nature of the binding of cytochrome *c* at the membrane−water interface was investigated by Langmuir−Blodgett (LB) and differential scanning calorimetric (DSC) techniques. The data obtained suggested that the protein was surface bound with minimal penetration into the membrane. LB studies were also used to probe the orientation of the trianionic porphyrin moiety at the membrane surface, and an edge-on orientation was inferred from the data. The formation of a stable vesicular system was confirmed by the formation of well-defined DSC thermograms. Phase separation was observed at high porphyrin:lipid ratios. Electron transfer from the Mn(II) in the membrane interior to the surface bound *ferri*cytochrome *c* was investigated, as a probe both for spatial definition of the ensemble and for the elucidation of electron transfer mechanism in the genre of weakly coupled systems over large distances. Trianionic Zn porphyrins with varying tether lengths (12, 8, and 4 carbons) were used. The electron transfer rate was found to be first order and independent of the tether length, indicative of medium mediated electron transfer via multiple pathways. Comparison to similar systems in the literature yielded a predicted distance of ∼23 Å between the Mn and Fe centers in DMPC/DPPC vesicles. This distance suggested that the protein was surface bound to the membrane and separated from the Mn porphyrin by the thickness of one leaflet of the phospholipid bilayer. In thinner DLPC vesicles the predicted increase in the electron transfer rate was observed. Additionally, electron transfer was observed to be bimolecular in systems where trianionic porphyrins lacking the imidazole tether were used to recruit the cytochrome *c*.

Introduction

Membranes are ubiquitous in biological systems.[1] In addition to defining the boundaries of the cell and subcellular organelles, membranes create a semipermeable filter which maintains chemical gradients and provides the structural foundation for the construction of pumping and signaling devices. Membrane directed protein self-assembly, cell surface recognition, and the regulation of membrane permeability are important aspects of respiration, photosynthesis, neurotransmission, and cell trafficking pathways. The biochemistry of membranes is also a fundamental issue in the pharmacology of drug delivery and drug design.[1b] Hence, studies on model membrane systems and methods of constituting complex molecular ensembles have important implications in diverse areas of cellular chemistry, biology, and medicine.

Compared to the art of organic synthesis, the use of weak, intermolecular forces to assemble large, multicomponent aggregates by design is in its infancy.[2] We have sought to explore the deployment of artificial hemes in phospholipid vesicles to extend the limits of membrane-directed self-assembly in a model system. Synthetic porphyrins have a number of attributes in this regard. They are large, conformationally restricted molecules which bear close structural resemblance to chlorophylls and the cytochromes.[3a] They can be designed to be hydrophobic, hydrophilic, or amphiphilic via convenient syntheses. Further, a family of richly developed porphyrin spectroscopies can be advantageous in probing local structure even in complex arrays. Porphyrins exhibit high quantum efficiency in their photochemistry and relatively long lifetimes of their excited states and offer an ease of spectroscopic monitoring.[3b] Finally, metalloporphyrins exhibit coordination chemistry, redox be-

* To whom correspondence should be addressed.

[⊗] Abstract published in *Advance ACS Abstracts,* February 15, 1996.

(1) (a) Voet, D. B.; Voet, J. G. *Biochemistry*; Wiley: New York, 1990; 528−557. An excellent basic text with separate chapters dedicated to lipids and membranes, photosynthesis, and respiration, with leading references. (b) An area of intense research, for which only a few examples are listed here: Schreier, H.; Ausborn, M.; Guenther, S.; Weissig, V.; Chander, R. *J. Mol. Recog.* **1995**, *8*, 59. Chikhale, P. J.; Marvanyos, E.; Bodor, N. S. *Cancer Biother.* **1994**, *9*, 245. Toth, I. *J. Drug. Targeting* **1994**, *2*, 217.

(2) (a) *Molecular Recognition*: *Chemical and Biochemical Problems*; Roberts, S. M., Ed.; Royal Society of Chemistry: Cambridge, 1989. (b) *Molecular Recognition*: *Chemical and Biochemical Problems II*; Roberts, S. M., Ed.; Royal Society of Chemistry: Cambridge, 1992.

(3) (a) The crystal structure for bovine cytochrome *c* oxidase has just been reported, and a more detailed understanding of complex membrane−protein ensembles is now at hand. See: Tsukihara, T.; Aoyama, H.; Yamashita, E.; Tomizaki, T.; Yamaguchi, H.; Shinzawa-Itoh, Nakashima, R.; Yaono, R.; Yoshikawa, S. *Science* **1995**, *269*, 1069. (b) Kalyansundaran, K. *Photochemistry of Polypyridines and Porphyrin Complexes*; Academic Press Limited: London, 1992. (c) *Cytochrome P-450*: *Structure, Mechanism and Biochemistry*; Ortiz de Montellano, P. R., Ed.; Plenum Press: New York, 1986.

0002-7863/96/1518-2347$12.00/0

havior, and catalysis which can serve as functional criteria for these model constructs.[3c]

The ordered nature of model membrane environments allows the compartmentalization of electron donors and acceptors, the facile introduction of relay molecules, and with proper design, control of the orientation of individual components with respect to one another.[4] Thus, membrane self-assembly offers a complementary approach to the construction of model electron transfer devices since the tedious design and construction of spatially defined, single-molecule systems can be replaced by the coordinated interactions of smaller units.

We have developed a membrane-binding steroidal porphyrin[5] which has been shown to span phosphatidylcholine (DMPC/DPPC) membranes, placing the porphyrin macrocycle in the middle of the bilayer with its plane perpendicular to the membrane normal. The porphyrin disposition was confirmed by oriented Cu(II) EPR spectroscopy, and its distance from the aqueous−lipid interface was inferred from the length of an amphiphilic tethered ligand required to reach from the aqueous interface to the metalloporphyrin center.[5b] Striking catalytic selectivities observed for steroid hydroxylation and epoxidation in these vesicular ensembles confirmed the orientation deduced by spectroscopic means.[5] Subsequently, we developed a model system in which electron transfer from the membrane-associated flavoprotein pyruvate oxidase to a Mn(III) steroidal porphyrin was mediated by a synthetic amphiphilic flavin which served as an electron shuttle. This reconstituted, semibiotic system was shown to effect hydrocarbon oxygenation.[6]

In a recent paper, we reported the construction of a model system designed to probe the nature of electron transfer between cytochrome *c* recruited to a membrane surface and a redox center embedded within a phospholipid bilayer at an approximately known distance.[7] A key structural feature of this ensemble was the design of the recruiter porphyrin which anchored itself to the manganese porphyrin center via ligation and was shown to bind cytochrome *c* at the membrane surface through electrostatic interactions.[8,9] The rate of electron transfer observed within this membrane ensemble and comparisons to rates for similar systems in the literature[7] yielded a predicted distance of 22−23 Å between the Mn and Fe centers. This distance suggested that cytochrome *c* in these constructs resides at the surface of the membrane, separated from the Mn porphyrin only by the thickness of one leaflet of the phospholipid bilayer (∼20 Å) as presented in Figure 1.[5b,7,10]

Here we describe a more complete analysis of this model membrane system. The nature of the binding of cytochrome *c* to its membrane surface receptor has been probed with fluorescence spectroscopy and Langmuir−Blodgett and differential calorimetric techniques. Variations in the rate of electron transfer between the membrane-bound manganese(II) porphyrin and *ferri*cytochrome *c* have been studied as a function of the structure of the tether and the thickness of the intervening phospholipid. The data obtained indicate that the system behaves as a single, unimolecular ensemble, that cytochrome *c* binds to its receptor with minimal perturbation or invasion of the membrane surface, and that a shorter *lipid* increased the rate of electron transfer from the Mn(II) center in the middle of the membrane to the surface-associated *ferri*cytochrome *c* in a predictable manner whereas the length of the intervening tether had little effect.

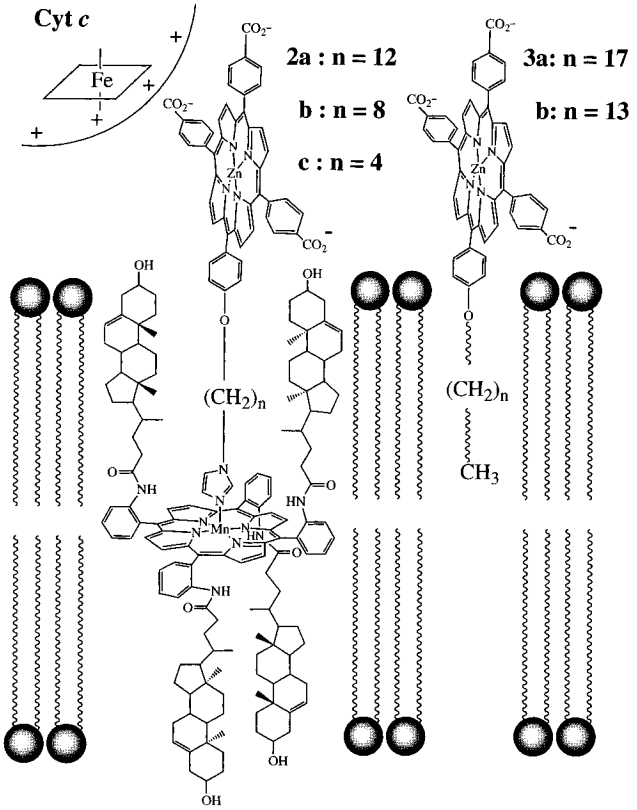

Figure 1. Ternary construct showing **1**−**2**−cytochrome *c*. Compounds **3a**,**b** are depicted at the right.

Results

Synthesis of Porphyrins. The membrane spanning Mn(III) porphyrin **1** (MnChPCl) was prepared as previously described.[5] The syntheses of the imidazole-tailed zinc (carboxyphenyl)-porphyrins **2a**−**c** (ZnTCImP) have also been reported.[7] The amphiphilic porphyrins **3a**,**b** were prepared as previously described.[8] The structures of **1**, **2**, and **3** are shown in Figure 1.

Formation of Vesicles and Assembly of Multicomponent Complexes. Initial efforts were focused on membrane self-assembly and spectroscopic analysis of the MnChPCl−ZnTCImP−cytochrome *c* ternary complex (**1**−**2**−cytochrome *c*) in phosphatidylcholine vesicles. This construct is depicted in Figure 1, and the assembly process described below is shown in Scheme 1.

Formation of the Binary 1−2 Complex. Vesicular suspensions of a mixture of dipalmitoylphosphatidylcholine (DPPC) and dimyristoylphosphatidylcholine (DMPC) (80:20) were prepared by sonicating a thin film of the lipids in phosphate buffer at pH 8. Dilaurylphosphatidylcholine (DLPC) vesicles

(4) For examples of biomimetic electron transfer in membranes see: (a) Fuhrhop, J.-H.; Matieu, J. *Angew. Chem., Int. Ed. Engl.* **1984**, *23*, 100. (b) Calvin, M. *Acc. Chem. Res.* **1978**, *11*, 369. (c) Moore, T. A.; Gust, D.; Moore, A. L.; Bensasson, R. V.; Seta, P.; Bienvenue, E. In *Supramolecular Photochemistry*; Balzani, V., Ed.; D. Reidel Publishing Co.: Holland, 1987. (d) Katigi, T.; Yamamura, T.; Saito, T.; Sasaki, Y. *Chem. Lett.* **1981**, 5030. (e) Moss, R. A.; Schreck, R. P. *J. Am. Chem. Soc.* **1985**, *107*, 6634. (f) Dannhauser, T. J.; Nango, M.; Oku, N.; Anzai, K.; Loach, P. A. *J. Am. Chem. Soc.* **1986**, *108*, 5865. (g) Gust, D.; Moore, T. A. *Science* **1989**, *244*, 35.

(5) Groves, J. T.; Neumann, R. *J. Am. Chem. Soc.* **1987**, *109*, 5045. (b) Groves, J. T.; Neumann, R. *J. Am. Chem. Soc.* **1989**, *111*, 2900. (c) Groves, J. T.; Neumann, R. *J. Org. Chem.* **1988**, *53*, 3891.

(6) Groves, J. T.; Ungashe, S. B. *J. Am. Chem. Soc.* **1990**, *112*, 7796.

(7) Groves, J. T.; Fate, G. F.; Lahiri, J. *J. Am. Chem. Soc.* **1994**, *116*, 5477.

(8) Ungashe, S. Ph.D. Thesis, Princeton University, 1991.

(9) (a) Clark-Ferris, K. K.; Fisher, J. *J. Am. Chem. Soc.* **1985**, *107*, 5007. (b) Zhou, J. S.; Granada, E. S. V.; Leontis, N. B.; Rodgers, M. A. J. *J. Am. Chem. Soc.* **1990**, *112*, 5074.

(10) (a) Elbers, P. F.; Ververgaert, J. T. *Cell. Biol.* **1965**, *25*, 375. (b) Engleman, D. M. *J. Mol. Biol.* **1970**, *47*, 115.

Scheme 1

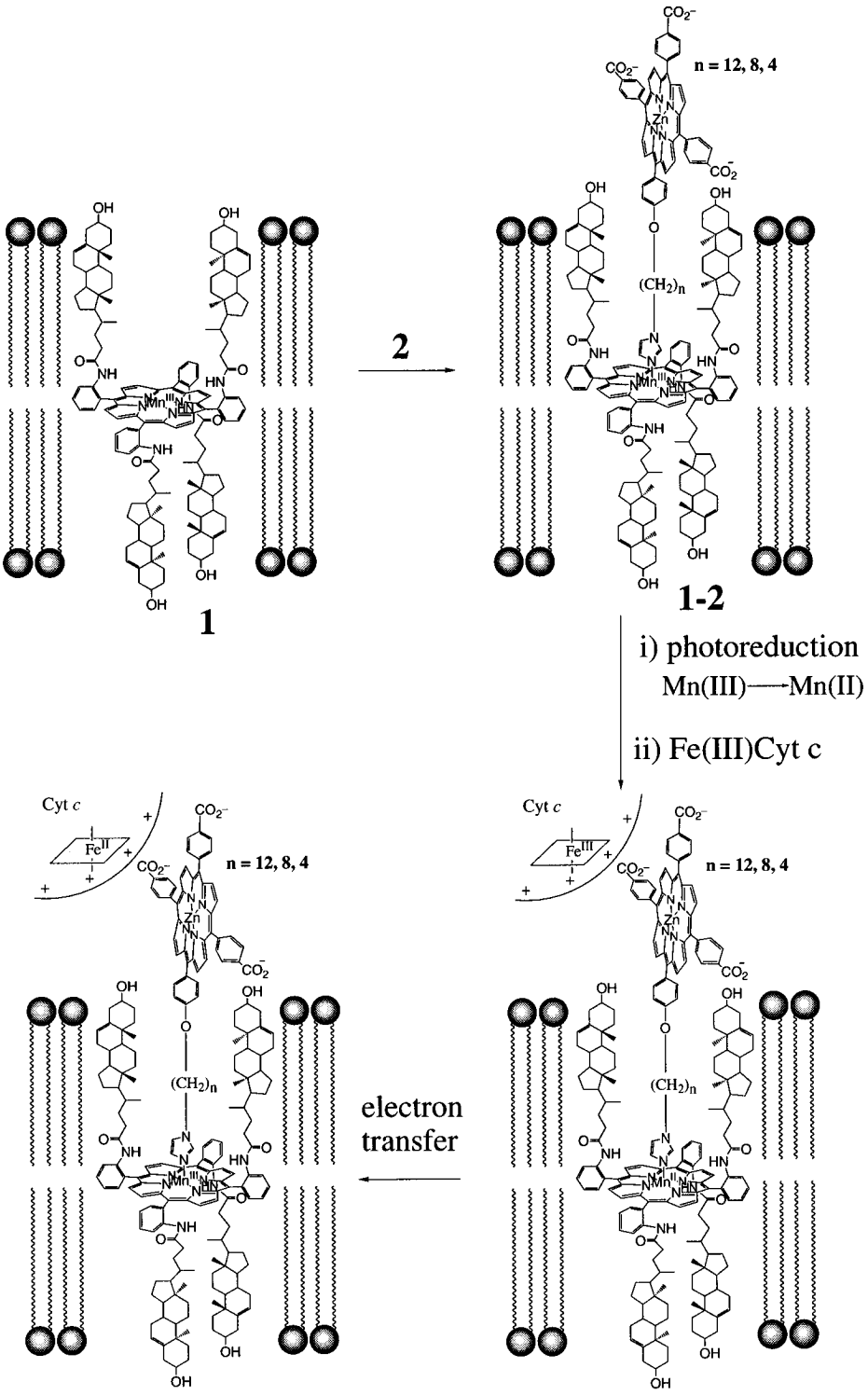

were prepared in a similar manner using pure lipid. Vesicular suspensions doped with the steroidal porphyrin Mn^{III}ChPOH (**1**) were formed upon sonication of a thin film of a lipid−porphyrin mixture with buffer. The formation of small, unilamellar vesicles (SUV), approximately 300 Å in diameter, was confirmed by transmission electron microscopy.

The amphiphilic zinc porphyrins **2** and **3** were added as 1:1 MeOH/water solutions to the preformed vesicular suspensions. Size exclusion chromatography of the vesicular mixture on Sepharose 4B and analysis of the eluting fractions by UV absorbance spectroscopy showed that both components **1** (474 nm) and **2** (or **3**) (430 nm) eluted with the lipid fraction (300 nm), thus confirming the binding of **2** (and **3**) to the lipid phase (Figure 2).

Effects of the Ligating Imidazole. Differences in the Behavior of 2 and 3. It was important to establish that ligation to form the binary **1**−**2** construct had occurred as anticipated. While the coelution of **1** with **2** showed that both were bound to the lipid phase, that alone did not provide evidence for the interaction between the Mn(III) center in **1** and the terminal imidazole of **2**. It was therefore necessary to find spectroscopic differences between the Zn porphyrins **2** and **3** (lacking the imidazole terminus on the hydrophobic tether) in their interactions with the Mn(III) porphyrin **1**.

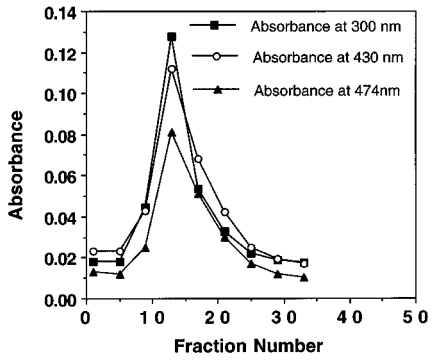

Figure 2. Size-exclusion chromatography on Sepharose 4B showing the elution of DPPC/DMPC (4:1) vesicles monitored by its absorbance at 300 nm, Mn(III)ChP(OH) (**1**) at 474 nm, and zinc porphyrin **2b** at 430 nm. The eluent was 5 mM phosphate buffer at pH 8.0. The preparation of vesicles is described in the Experimental Section.

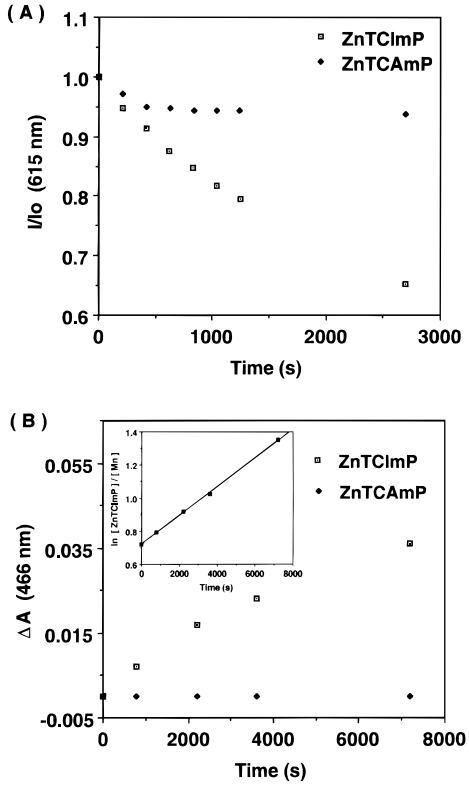

Figure 3. Spectroscopic evidence for ligation of **2** to **1**. (A) Time course for the decrease in fluorescence intensity of **2a** (ZnTClmP) and **3** (ZnTCAmP) upon addition to a vesicular solution containing **1** (1 mM) in phosphate buffer (pH 8, 5 mM). (B) Hypochromicity in the UV spectrum (466 nm) versus time upon the addition of **2a** to **1** (5 μM), under the same buffer conditions. There was no change upon the addition of **3a** to **1**. The inset is a second-order plot of the kinetics of the ligation ($k = 20$ M^{-1} s^{-1}).

The fluorescence of the zinc porphyrins **2** and **3** provided a convenient tool to monitor their interactions with vesicles containing **1**. The time course of the fluorescence intensity for the Zn porphyrins **2a** and **3a**, upon addition to a vesicular solution of **1**, showed distinct differences as shown in Figure 3A. Both **2a** and **3a** showed a rapid, initial decrease in fluorescence intensity of about 5%. The plateau reached in the quenching of **3a** was attained in a short time. By contrast, a continuing decrease in the fluorescence of **2a** was observed over ~45 min. Moreover, the degree of quenching for **2a** was considerably higher, ~45%. These observations are consistent with the insertion of the hydrophobic tails for both amphiphilic zinc porphyrins in the initial phase and then a slower diffusion of **2a** within the membrane to finally coordinate to the Mn(III) porphyrin **1** via its terminal imidazole. The enhanced quenching for **2a** is indicative of a closer average distance between the Zn and the Mn. For **2a**, the ligation to the Mn(III)[7,11] would prevent any lateral diffusion, and hence, the distance between the Zn and the Mn would be restricted to the width of half the bilayer. However, the Zn porphyrin **3a**, being free to diffuse within the membrane, would be on average further away from the Mn (See Discussion and Figure 11).

The ligation of the imidazole tether of **2** could also be detected by simultaneously monitoring changes in the UV spectrum of the Mn(III) porphyrin **1**. The addition of **2a** to a vesicular suspension of **1** caused changes in the visible spectrum at 466 nm as shown in Figure 3B. The ligation rate was observed to be second order as expected, and proceeded with a rate constant of 20 M^{-1} s^{-1} (Figure 3B, inset). No such time-dependent spectral change was observed when **3a** was added to a vesicular solution of **1**.

Cytochrome *c* Binding to the Binary 1−2 Complex To Form the Ternary Construct. The addition of cytochrome *c* to a vesicular solution containing the zinc porphyrins **2** and **3** resulted in a red shift of the Zn Soret from 430 to 432 nm, with a concomitant blue shift in the cytochrome *c* from 410 to 408 nm. The red shift of the Zn porphyrin chromophore was also accompanied by hypochromicity, and this was used as a spectral probe to establish the stoichiometry and the binding constant between **2** (or **3**) and cytochrome *c*. Spectral titrations of the cytochrome *c* to the **1**−**2** vesicular complex resulted in increased hypochromicity upon addition of aliquots of the protein to the zinc porphyrin, and this spectral change was found to plateau off after the addition of approximately 1 equiv of cytochrome *c*. A plot of the spectral change as a function of added cytochrome *c* resulted in a point of inflection at a 1:1 ratio of the protein to the Zn porphyrin,[7−9] as seen in Figure 4A. These observations are consistent with the formation of a 1:1 complex with cytochrome *c*, with a binding constant of $\sim 5 \times 10^6$ M^{-1}.[12]

The addition of cytochrome *c* resulted in the quenching of the Zn fluorescence (in **2** and **3**), and a Stern−Volmer plot of the quenching is indicative of tight binding[13] between cytochrome *c* and **2** (Figure 4B).

Monolayer Studies. Research on Langmuir−Blodgett (LB) monolayers[14] has provided valuable information about lipid miscibility and headgroup orientation and insights into the behavior of lipid associated enzymes. LB techniques provide

(11) (a) Axial ligation of nitrogenous bases to Mn porphyrins is well documented. For a review see: Boucher, L. J. *Coord. Chem. Rev.* **1972**, *7*, 289. (b) Mn(II) porphyrins form 1:1 complexes with coordinating nitrogenous ligands like imidazole. See: Hoffman, B. M.; Szymanski, T.; Brown, T. G.; Basolo, F. *J. Am. Chem. Soc.* **1978**, *100*, 7253. (c) Gonzalez, B.; Kouba, J.; Yee, S.; Reed, C. A.; Kirner, J. F.; Scheidt, W. R. *J. Am. Chem. Soc.* **1975**, *97*, 3247. (d) Kelly, S. L.; Kadish, K. M. *Inorg. Chem.* **1982**, *21*, 3631.

(12) At a constant concentration of the Zn porphyrin **2**, its hypochromicity ΔA as a function of *ferri*cytochrome *c* concentration could be described by the quadratic equation (assuming a 1:1 complex) $\Delta A = \Delta A_\infty/2P[C + P + 1/K_a - \{(C + P + 1/K_a)^2 - 4CP\}^{1/2}]$ where K_a is the equilibrium association constant, C is the concentration of cyt *c* and P is the concentration of **2**. The average value of K_a obtained is $(5 \pm 3) \times 10^6$ M^{-1}. See: Erman, J. E.; Vitello, L. B. *J. Biol. Chem.* **1980**, *255*, 6224.

(13) Stubbs, C. D.; Williams, B. W. In *Topics in Fluorescence Spectroscopy*; Lakowicz, J. R., Ed.; Plenum Press: New York, 1992; Vol. 3.

(14) (a) Roberts, G., Ed. *Langmuir-Blodgett Films*; Plenum Press: New York, 1990. An excellent book on the diverse chemistry of Langmuir−Blodgett films, with leading references. The behavior of phosphatidylcholine monolayers is described in Chapter 6. (b) Ishikawa, Y.; Kunitake, T. *J. Am. Chem. Soc.* **1991**, *113*, 621. (c) Cherry, R. J.; Kwan, H.; Chapman, D. *Biochim. Biophys. Acta* **1972**, *267*, 512. (d) Bull, R. A.; Bulkowski, J. E. *J. Colloid Interface Sci.* **1983**, *92*, 1. (e) Liu, M. D.; Leidner, C. R.; Facci, J. S. *J. Phys. Chem.* **1992**, *96*, 2804. (f) Scheidt, W. R. *Acc. Chem. Res.* **1977**, *10*, 1584.

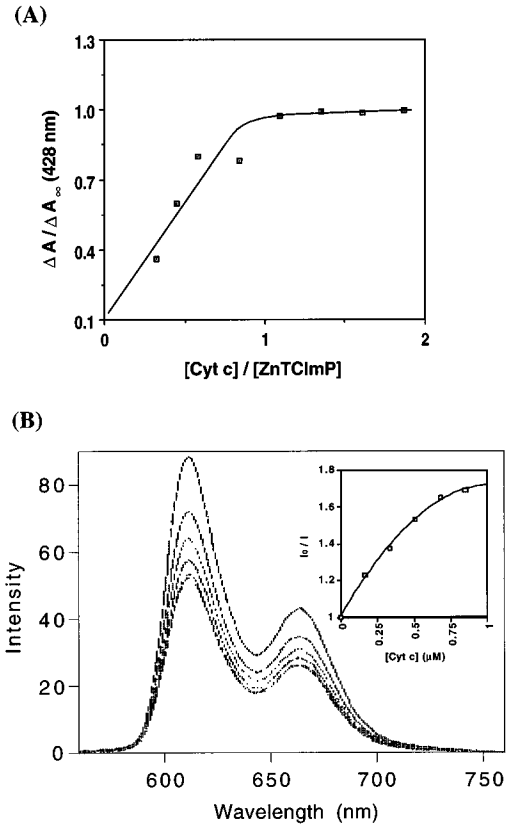

Figure 4. (A) UV difference titration of **2a** with cytochrome *c*, indicating the formation of a 1:1 complex with a high binding constant ($K_a \sim 5 \times 10^6$ M^{-1}). Concentration of **2a** was 1 μM (in 5 mM phosphate buffer, pH 8). (B) Fluorescence quenching (emission spectra) of **2a** by cytochrome *c*. The inset shows a Stern−Volmer plot of the quenching data, also indicating strong binding. The concentration of **2a** was 0.6 μM in phosphate buffer (5 mM, pH 8). The excitation wavelength was 434 nm.

an ideal means to prepare lipid assemblies with a high degree of structural definition. The area occupied by a molecule at the lipid−water interface in a monolayer can be used to determine its orientation in a membrane.[14]

Porphyrin ring orientations at lipid−water interfaces have been investigated by anisotropic EPR,[5b,14b] polarized UV spectroscopy,[14c] and monolayer studies.[14d] The orientation of the porphyrin at the membrane interface, parallel, perpendicular, or random, is known to depend on the arrangement of the charges on the periphery of the porphyrin ligand.[14b] The orientation of the trianionic Zn porphyrin **3** at the lipid−water interface was investigated by LB studies.

Figure 5 represents the surface pressure vs molecular area (π−A) isotherms of Langmuir monolayers of DPPC and DPPZ/ZnTcAmP (**3a**). The features of the DPPC isotherm closely resemble previous reports.[14a,e] At large areas (>100 Å^2/molecule) the film is in an expanded (E) state. Upon compression, the film undergoes a transition from the E phase to the lipid expanded (LE) phase (90-90 Å^2/molecule). Further compression leads to the liquid expanded/liquid condensed (LE/LC) transition (60 Å^2/molecule), to the LC phase at ∼55 Å^2/molecule, and finally to a solid condensed phase (SC) at areas less than ∼47 Å^2/molecule. If the second linear portion of the isotherm corresponding to the LC to SC phase transition is extrapolated to zero surface pressure, the intercept gives the area per DPPC molecule that would be expected for the hypothetical state of an uncompressed close-packed layer. This value of ∼58 Å^2/molecule, referred to as the extrapolated area,

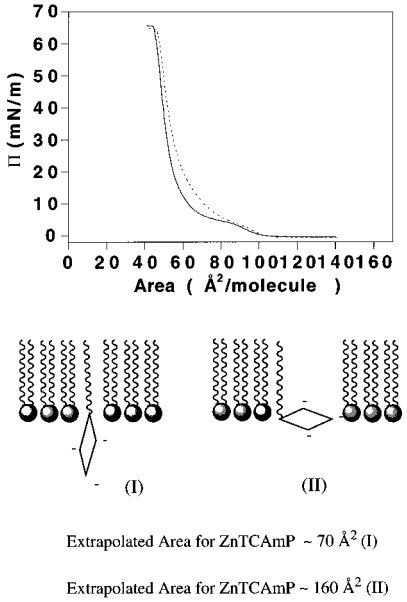

Figure 5. Surface pressure (π)/area isotherms of DPPC (—) and DPPC/ZnTCAmP (**3a**) (8:1) (···). The subphase was 5 mM phosphate buffer (pH 7.6). The films were compressed at the rate of 20 mN/m.

is a measure of the area occupied by each DPPC molecule in a compact film.

Isotherms recorded on a LB trough for monolayers of DPPC doped with 12.5% ZnTCAmP (**3a**) resulted in an increase in the mean molecular area from ∼58 to ∼61 Å^2. It can be seen, however, that the π−A isotherm had essentially the same characteristics, indicating that the dopant porphyrin had not significantly perturbed the DPPC monolayer at this ratio. Since the porphyrin orientation (as measured by its extrapolated area at the lipid−water interface) in bulk DPPC was the subject of this investigation, the smallest porphyrin:lipid ratio at which one could accurately measure the difference in the area upon the addition of the porphyrin was used. Assuming additive mixing ($A = A_1{*}x_1 + A_2{*}x_2$, where $A_i{*}$ and x_i represent the mean molecular areas and the mole fractions of the respective pure lipids), this yields an extrapolated area of ∼70 Å^2 for **3**. On the basis of structural data for tetraphenylporphyrins,[14d,f] extrapolated areas of ∼160 and 70 Å^2 would be expected for flat and vertical orientations, respectively, for the porphyrin macrocycle. Thus, the porphyrin headgroup in **3** must be oriented with its plane approximately perpendicular to that of the membrane surface as shown in Figure 5.

It was also important to determine whether the interaction between **3** and the cytochrome *c* occurred within or at the surface of the membrane. Two different monolayer techniques were employed to answer this question. First, if the monolayer film was allowed to incubate with cytochrome *c* added to the aqueous subphase, π−A isotherms could be used to infer lipid−cytochrome *c* interactions. An increase in the molecular area would imply that the protein had penetrated the lipid since each protein molecule would now occupy a finite area at the lipid−water interface. Hence, the lipid would undergo transitions to more condensed phases at lower compressions, corresponding to higher extrapolated areas. Second, the penetration of a protein into a membrane could be measured by monitoring changes in the surface pressure of the lipid monolayer versus time after injection of the protein into a stirred subphase beneath the surface monolayer. An increase in the surface pressure would imply protein penetration. The extent of penetration is dependent not only on the protein−lipid interaction but also on the compression state of the monolayer. Typically, these experi-

ments are carried out in partially compressed monolayers, since protein penetration is inhibited in stiff fully compressed monolayers.[15a]

The nature of the monolayer−protein interactions was addressed by studying the effect of the cytochrome *c* on the isotherms for the porphyrin doped monolayers. Isotherms recorded for DPPC/ZnTCAmP (8:1) (Figure 5), showed almost no change when cytochrome *c* was present in the subphase. By contrast, when an 8:1 mixture of DPPC and stearic acid was compressed under identical conditions, there was a ∼21% *increase* in the mean molecular area when cytochrome *c* was added to the subphase. This implies that when the lipid is doped with the porphyrin, the cytochrome *c* penetration is much less significant than when it is doped with anionic lipids such as stearic acid. Since cytochrome *c* forms a strong 1:1 complex with porphyrin doped membranes, it can be inferred that the complex was formed at or just above the membrane surface.

Cytochrome *c*−lipid interactions were also investigated by observing the increase in surface pressure upon protein penetration. When cytochrome *c* was injected beneath the surface of a partially compressed monolayer, the resulting increase in the surface pressure was lower when the vesicles were doped with **3a** than with pure lipid, as shown in Figure 6. From these observations we could infer that the interaction of the cytochrome *c* with **3a** did not proceed with a large penetration into the membrane, and that the porphyrin was limiting the penetration of the protein by the formation of a stable complex on the membrane surface. The slight increase observed could be attributed to the peripheral interactions of the bulk protein with the surface of the membrane.

Thus, both approaches support the view that the interaction with cytochrome *c* did not occur with significant membrane penetration but was rather a strong surface interaction with the porphyrin doped lipid. This result is contrary to that generally obtained for neutral lipids with negatively charged dopants such as phosphatidic acid.[15] Typically, a large increase in surface pressure was observed upon doping with the anionic molecules, indicative of enhanced penetration by the cytochrome *c*. This was attributed to the larger size of the phosphatidylcholine headgroup vis-a-vis that for phosphatidic acid.[15b] We attribute the decreased penetration to the large porphyrin headgroup extending into the aqueous boundary layer above the phosphatidylcholine moiety and forming an electrostatically stabilized complex.

Differential Scanning Calorimetry (DSC). DSC has been one of the most widely used methods for studying the thermal behavior of lipids.[16] Thus, the effects of amphiphilic porphyrins as dopants on vesicle stability were investigated. It was expected that there would not be significant changes in the lipid stability at the low porphyrin to lipid ratio used for the subsequent electron transfer experiments. However, it was necessary to ensure this because a stable vesicular system was central to the formation of spatially well-defined constructs. As we have previously described, the Mn steroidal porphyrin **1** caused broadening and shifts in the lipid DSC thermogram.[5b] Accordingly, the effect of the amphiphilic Zn porphyrin **3b** in pure DMPC vesicles was investigated. Secondly, DSC was used to probe the surface interaction of cytochrome *c* with vesicles doped with **3b**. Protein penetration into the membrane would be expected to reduce the interactions between neighboring lipid molecules and, hence, would decrease the stability of the membrane. On the other hand, surface lipid−protein interactions would not reduce membrane stability.

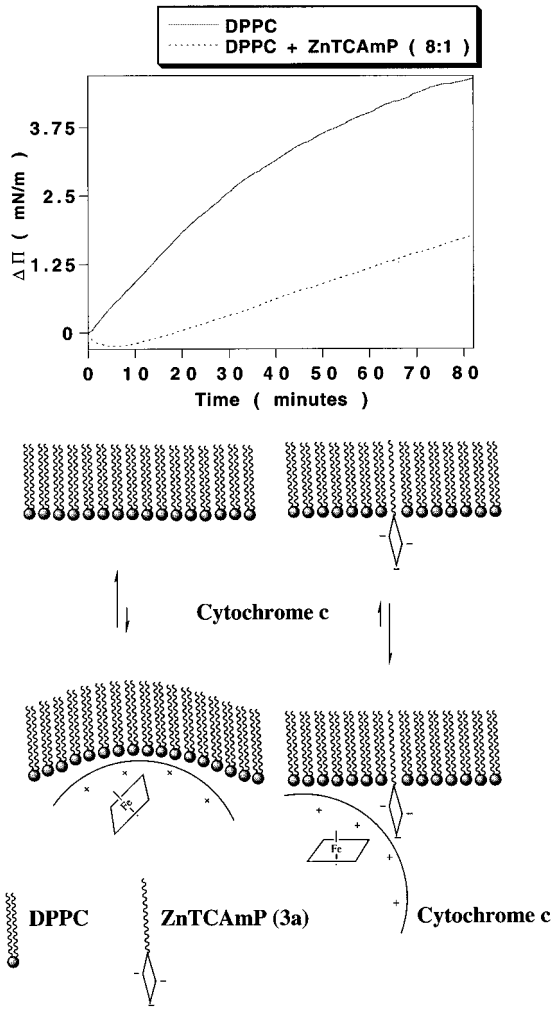

Figure 6. Membrane penetration as measured by the change in surface pressure ($\Delta\pi$) with time, after cytochrome *c* was injected under the surface of a partially compressed monolayer. The monolayers were compressed to 10 mN/m, and 10 μL of 100 μM cytochrome *c* was injected as the subphase was stirred from the underneath at a constant speed of 12 rpm. The final ratio of the protein to the lipid mixture was 1:1.

The excess heat capacity functions of DMPC (trace a), DMPC−ZnTCAmP (**3b**) (120:1) (trace b), DMPC−ZnTCAmP (12:1) (trace c), and DMPC−ZnTCAmP (12:1) with added cytochrome *c* (trace d) are shown in Figure 7. The transition characteristics for these lipid systems are tabulated in Table 1. As can be seen from a comparison of traces a and b, there is little change in the thermotropic behavior of DMPC upon doping with the amphiphilic porphyrin. Clearly, since the electron transfer experiments described below were carried out at even higher ratios of DMPC:ZnTCAmP (∼650:1), it would be reasonable to assume that there was negligible perturbation of the lipid structure at such low concentrations of the porphyrin. However, in order to study the effect of cytochrome *c*, we used a much higher concentration of the porphyrin, since the anionic porphyrin was responsible for recruiting the cytochrome *c* to the membrane (a ratio of 12:1 (DMPC/ZnTCAmP (**3b**)) was used). As was evident (trace c), the pretransition had completely disappeared, and phase separation seemed to occur, with one phase (which had a T_m similar to DMPC, 24.5 °C) having a broad transition with a cooperative unit (cu) of ∼20, and another phase with a sharp transition at 22.7 °C (cu ∼450). We interpreted the broad transition as being that for pure DMPC,

(15) (a) Dawson, R. M. C.; Quinn, P. J. *Biochem. J.* **1969**, *113*, 791. (b) Teissie, J. *Biochemistry* **1981**, *20*, 1554.

(16) (a) Chapman, D. *Biological Membranes*; Academic Press: New York, 1968; Vol. 1. (b) Blume, A. *Thermochimica Acta* **1991**, *193*, 299.

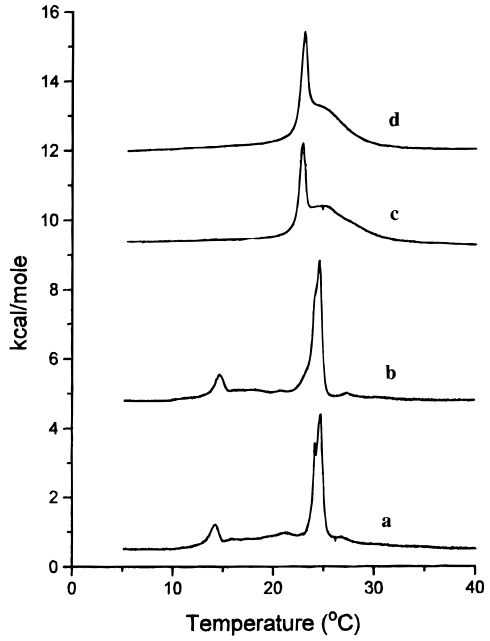

Figure 7. Heat capacity curves for DMPC (trace a), DMPC/ZnTCAmP (120:1) (trace b), DMPC/ZnTCAmP (12:1) (trace c), and DMPC/ZnTCAmP + cyt *c* (DMPC:ZnTCAmP:cyt *c* = 12:1:1) (trace d). All the scans were carried out at a scan rate of 20 °C/h, at a final lipid concentration of 2.7 mM, in 5 mM phosphate buffer. The vesicular solution for trace d was incubated for 1 h after the addition of the protein. All the DSC experiments were carried out using the amphiphilic porphyrin **3b**.

Table 1. Transition Properties of the Various Lipid Mixtures

lipid	T_{m_1} (°C)	ΔH_1 (kcal mol^{-1})	T_{m_2} (°C)	ΔH_2 (kcal mol^{-1})
DMPC	14.3	1.0	24.4	5.4
DMPC/ZnTCAmP (120:1)	14.6	1.0	24.4	5.5
DMPC/ZnTCAmP (12:1)			22.7, 24.5	1.7, 4.1
DMPC/ZnTCAmP/cyt *c* (12:1:1)			23.2, 24.4	2.5, 4.2

with the decreased cooperativity resulting from the presence of the dopant. The sharp transition could be that for a porphyrin rich phase though we were unable to explain the highly cooperative nature of the transition. Such lateral phase separations[17] in mixtures of charged and neutral lipids are to be expected due to the large differences in both size and charge between the DMPC and the porphyrin. Interestingly, the addition of cytochrome *c* resulted in an increase in the T_m of the putative "porphyrin rich" phase to 23.2 °C with an increase of ∼1 kcal/mol in the enthalpy of the transition. We did not see any such increase in T_m or the transition enthalpy (ΔH) for the "DMPC rich" phase, though the transition appeared less broad. Electrostatic surface interactions are known to often lead to an increase in the ΔH and the T_m.[16] Hence, these results affirmed the surface binding of the recruited protein, with little penetration into the bilayer.

Electron Transfer Reactions. Electron transfer reactions within the ternary **1**−**2**−cytochrome *c* complex were examined both as an additional probe of the structure of these arrays and as a probe of the nature of the electron transfer event. The ensemble provides a bilayer limited distance between the redox centers, with the possibility of variation in the tether length of the "relay molecule" **2**. The system might thus seek to address the mechanism of electron transfer in a weakly coupled system,

(17) Shimshick, E. J.; McConell, H. M. *Biochemistry* **1973**, *12*, 2351. (b) Galla, H. J.; Sackmann, E. *Biochem. Biophys. Acta* **1975**, *401*, 509.

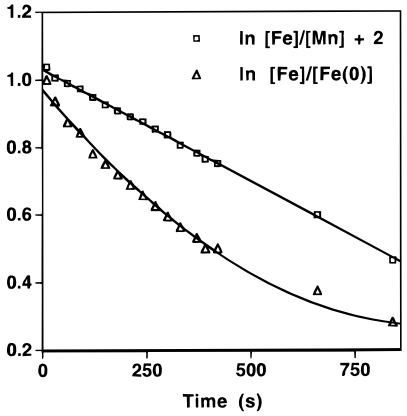

Figure 8. First- and second-order plots of electron transfer to *ferri*cytochrome *c* as monitored by the appearance of *ferro*cytochrome *c* at 550 nm and the disappearance of Mn(II) at 444 nm (for **3a**). From the first-order plot, at low concentrations of Fe(II), when [Mn(II)] ≫ [Fe(II)], one can estimate a pseudo-first-order rate constant of 3.8 × 10^{-4} s^{-1}.

at large distances and at a low driving force. These measurements were achieved by forming the Mn(III) binary **1**−**2** complex by incubation of the vesicular suspension for ∼2 h to ensure complete ligation and subsequent photoreduction of Mn(III) to Mn(II), thus providing a driving force of ∼0.30 eV for electron transfer from the Mn(II) to *ferri*cytochrome *c*. The redox couple was calculated, on the basis of the measured $E_{1/2}$ of the MnChPCl (**1**)−1-methylimidazole adduct[18] by cyclic voltammetry. The electron transfer, at such large distances, could be monitored by simple UV spectroscopy.

In a typical experiment, 1 equiv of **2** (or **3**) was added to 3 mL of a 3.33 mM solution of a 80:20 mixture of dipalmitoylphosphatidylcholine (DPPC) and dimyristoylphosphatidylcholine (DMPC) in phosphate buffer (5 mM, pH 8) containing 15 nmol of **1**. The ligation (for **2**) was complete in about 2 h, as evidenced by a plateau in the time course of fluorescence quenching of the zinc porphyrin **2** upon its addition to the vesicular mixture. Equilibrium quenching for **3** was complete in ∼5 min. The cuvette containing the reactants was degassed with argon for 1 h, and the Mn(III) porphyrin was subjected to photoreduction.[19] The progress of the photoreduction was monitored by the appearance of the Mn(II) porphyrin absorbance at 444 nm and the disappearance of the absorbance at 474 nm characteristic of Mn(III). At this point 10 μL of rigorously degassed 1 mM ferricytochrome *c* was added, and the formation of *ferro*cytochrome *c* was monitored by the appearance of Fe(II) at 550 nm in the visible spectrum.

The kinetic analysis of the electron transfer from Mn(II) to Fe(III) cytochrome *c* shows different molecularities for the ligated construct **2a** and the unligated **3a**. The electron transfer from Mn(II) to *ferri*cytochrome *c* was first order for the construct **2a**[7] (k = ∼10^{-3} s^{-1}) and second order for **3a** (with a rate constant of 1.57 M^{-1} s^{-1}), over several half-lives (Figure 8). The unimolecular kinetics in the case of **2a** provides strong kinetic evidence for the formation of a ternary **1**−**2**−cytochrome *c* complex. The change from unimolecular to bimolecular kinetics for **3a** is attributable to electron transfer from the Mn(II) to the independently diffusable **3a**−Fe(III)cytochrome *c* complex.

(18) The $E_{1/2}$ of **1** in the presence of 1-methylimidazole in CH_2Cl_2 was measured to be −0.28 V (vs SCE), or −0.04 V vs NHE. This would result in a redox couple for the Mn(II)−*ferri*cytochrome *c* system to be 0.30 V (vs NHE) [$E_{1/2}$ of the protein is 0.262 V (NHE)]. See: Taniguchi, V. T.; Ellis, W. R., Jr.; Cammarata, V.; Webb, J.; Anson, F. C.; Gray, H. B. *Adv. Chem. Ser.* **1982**, *201*, 51.

(19) Hendrickson, D. N.; Kinnaird, M. G.; Suslick, K. S. *J. Am. Chem. Soc.* **1987**, *109*, 1243.

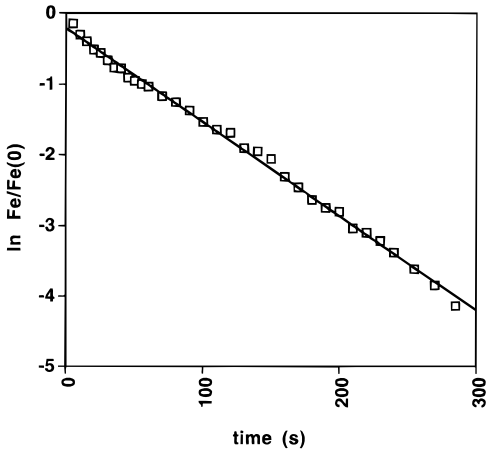

Figure 9. First-order plot of the formation of *ferro*cytochrome *c* (550 nm) in DLPC vesicles. Data shown for **2c**, $k = 1.46 \times 10^{-2}$ ($R^2 = 0.997$).

Table 2. Rates for Electron Transfer from Mn(II) to Fe(III)cytochrome *c* ($\times 10^{-3}$ s^{-1})[a]

	DPPC/DMPC vesicles			DLPC vesicles		
	2a ($n = 12$)	**2b** ($n = 8$)	**2c** ($n = 4$)	**2a** ($n = 12$)	**2b** ($n = 8$)	**2c** ($n = 4$)
k	1.91	2.00	1.79	15.0	14.0	15.1
$\ln k$	−6.26	−6.21	−6.32	−4.19	−4.26	−4.19

[a] The rates represent the average rates in each lipid system, as observed in three independent experiments.

We have reported that the electron transfer rate was independent of the tether length, but rather occurred at rates consistent with the bilayer limited distance between the redox centers.[7] We decided to probe electron transfer in smaller vesicles, to change the bilayer limited distance between the redox centers, and hence increase the rate of electron transfer. Electron transfer reactions in vesicles with the shorter DLPC lipid showed the expected first-order kinetics for **2a**, **2b**, and **2c**, at rates again independent of the length of the hydrocarbon tether. However, the rate obtained was ∼10 times faster than that observed in DPPC/DMPC vesicles. Figure 9 is a first-order plot of the formation of *ferro*cytochrome *c*, monitored by its appearance at 550 nm, when the cytochrome *c* was tethered *via* **2c** to **1**. The electron transfer rates for **2a**, **2b**, and **2c** in the two vesicular systems are tabulated in Table 2. The data clearly indicated that in a given vesicular assembly the rate of electron transfer was independent of the tether length, but dependent on the width of the vesicle bilayer (cf. Discussion).

Modeling Studies. Molecular modeling was carried out to determine whether the ligated Zn porphyrins were "long" enough to interact with the cytochrome *c*. The imidazole nitrogen was constrained to a 2 Å[20] distance from the Mn in the membrane spanning porphyrin. It was evident that the trianionic moiety was able to extend itself beyond the steroidal appendages even for the four-carbon tether in **2c**.

The computer graphic also shows the approximately perpendicular orientation of the amphiphilic porphyrin (**2b**) headgroup with respect to the plane of the membrane. The pertinent electrostatic interactions between the tricarboxy amphiphilic porphyrins and cytochrome *c* are those between the lysines around the solvent exposed heme edge of the cytochrome *c* and the carboxylates of the porphyrin **2**.[5,8,9] The results of kinetic studies on lysine single-modified derivatives and NMR investigations have implicated "site III"[21] (Lys 13, Lys 72, Lys 86) to have a high affinity for anionic reactants and to be kinetically the most relevant. Figure 10 highlights the side chains of the above lysines, and the carboxylates are represented by CPK models. The interactions between the two could occur between any three sets of the lysines that have the same topological symmetry as the trianionic porphyrin. In Figure 10, the lysines 86, 72, and 13 are shown to interact with the carboxylates (as implicated in the literature), though the flexible side chain of Lys 79 (instead of 13) might well be involved in the complexation. Experimental and modeling investigations have indicated that the two porphyrin rings are approximately perpendicular with a center to center distance of about 12 Å.[8,9b,22] The purpose of the computer graphic is to illustrate the basic features of the ternary assembly in a vesicular system. The modeling studies do not invoke the specific presence of the lipid though consideration of the lipid and other hydrophobic and steric interactions certainly must be important to obtain an accurate structural model.

Discussion

We have developed a biomimetic model system to study redox active heme arrays in phospholipid membranes. The design is based on molecular recognition, self-assembly, and the ability of membranes to compartmentalize components in an ordered manner. Kinetic and structural evidence has been obtained for a spatially well-defined system. The system may also lend insight into the nature of electron transfer mechanisms in the genre of weakly coupled systems over large distances.

The number of membrane spanning manganese porphyrin molecules (**1**) per vesicle in a typical assembly could be estimated to be ∼9 from the ratio of the lipid (10 μmol) to porphyrin (15 nmol).[23] While much higher concentrations of **1** could be tolerated in these vesicles, this level of loading was chosen to prevent overcrowding of the vesicle surface even when adorned with cytochrome *c*, a spherical protein with a diameter of ∼35 Å.[24]

The formation of the binary complex between **1** and the imidazole-tailed amphiphilic zinc porphyrin **2** was indicated by observing the distinct differences in spectroscopic behavior upon adding **2** or **3** (the amphiphilic porphyrin lacking the imidazole terminus) to vesicular suspensions of **1**. The formation of the ternary construct **1**−**2**−cytochrome *c* was also determined conveniently by fluorescence and UV spectroscopy. Interestingly, the interaction of the cytochrome *c* with the anionic porphyrin occurred within seconds, whereas the ligative **1**−**2** interaction developed over a much longer period (∼1 h). Thus, it is possible to form the binary **1**−**2** construct initially, add the

(20) Gonzales, B.; Kouba, J.; Yee, S.; Reed, C. A.; Kirner, J. F.; Scheidt, W. R. *J. Am. Chem. Soc.* **1975**, *97*, 3247. (b) Kirner, J. F.; Reed, C. A.; Scheidt, W. R. *J. Am. Chem. Soc.* **1977**, *99*, 2557.

(21) (a) Butler, J.; Chapman, S. K.; Davies, D. M.; Sykes, A. G.; Speck, S. H.; Osheroff, N.; Margoliash, E. *J. Biol. Chem.* **1983**, *258*, 6400. (b) Butler, J.; Davies, D. M.; Sykes, A. G.; Koppenol, W. H.; Osheroff, N.; Margoliash, E. *J. Am. Chem. Soc.* **1981**, *103*, 469. (c) Koppenol, W. H.; Margoliash, E. J. *J. Biol. Chem.* **1982**, *257*, 4426.

(22) (a) Pachence, J. M.; Amador, S.; Maniara, G.; Vanderkooi, J.; Dutton, P. L.; Blasie, J. K. *Biophys. J.* **1990**, *58* (2), 379. (b) Erecinska, M.; Blasie, J. K.; Wilson, D. F. *FEBS Lett.* **1977**, *76*, 235. (c) Ishikawa, Y.; Kunitake, T. *J. Am. Chem. Soc.* **1991**, *113*, 621. (d) Pelletier, H. J.; Kraut, J. *Science* **1992**, *258*, 1748.

(23) Assuming the surface area per headgroup to be 74 and 61 Å^2 in the inner and outer vesicle monolayers (Huang, C.; Mason, J. T. *Proc. Natl. Acad. Sci. U.S.A.* **1978**, *75*, 308), a vesicle diameter of 300 Å, and a bilayer width of 40 Å, the number of lipid molecules is ∼6000 per vesicle (at a ratio of 1.7 for the number of lipids in the outer vs inner shell, see: Huang, C. H.; Sipe, J. P.; Chow, S. T.; Martin, R. B. *Proc. Natl. Acad. Sci. U.S.A.* **1974**, *71*, 359 and Yeagle, P. L.; Hutton, W. C.; Martin, R. B.; Sears, B.; Huang, C. *J. Biol. Chem.* **1976**, *251*, 2110).

(24) Takano, T.; Kallai, O. B.; Swanson, R.; Dickerson, R. E. *J. Biol. Chem.* **1973**, *248*, 5234.

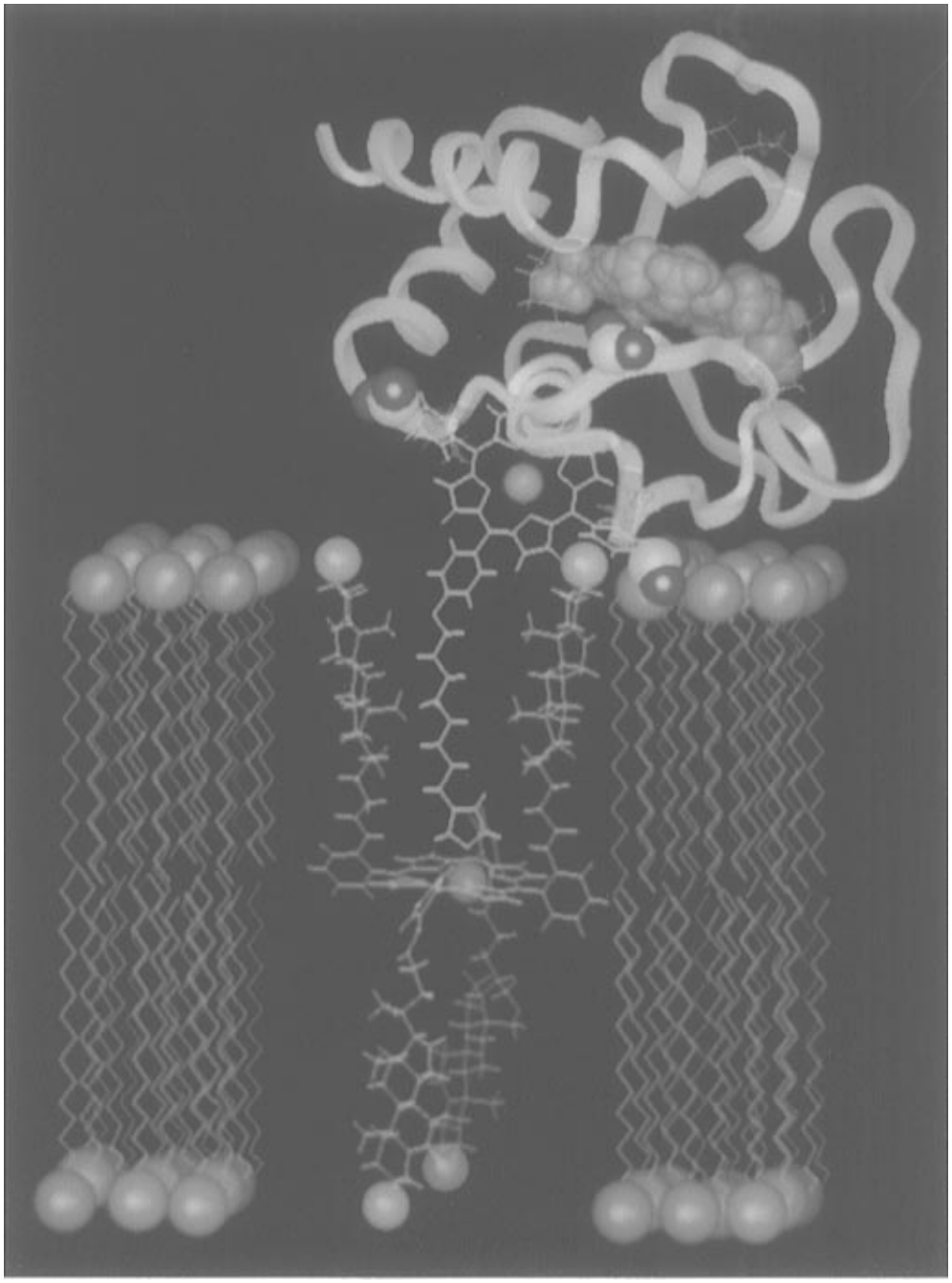

Figure 10. Computer graphic of the ternary system (**1**−**2b**−cytochrome *c*) in a membrane bilayer. The heme of the cytochrome *c* is shown in purple (CPK), and the carboxylates of **2b** along with the side-chains of the pertinent lysines around the solvent exposed heme edge are highlighted. The Mn(II) in **1** is 0.5 Å above the heme plane and is ligated to the imidazole with a Mn−N distance of 2 Å. The cytochrome *c* was rotated wrt the amphiphilic porphyrin such that energy minima were obtained; the graphic represents one such relative conformation. The flexible side chains of the lysines were also adjusted, and the final distances between the positively charged N atoms and the neighboring negatively charged O atoms of the porphyrins were 3.9 Å (lys 86), 2.3 Å (lys 13), and 2.6 Å (lys 72). The purpose of this graphic is to merely highlight the salient features of the ternary system and does not purport to be an accurate representation of the assembly.

cytochrome *c* to form the ternary complex, and then begin monitoring the electron transfer event without losing significant kinetic information. The rate of electron transfer was found to have a half-life of at least 400 s in DMPC/DPPC vesicles and ∼30 s in DLPC vesicles. Hence, the reaction progress could be measured conveniently by UV spectroscopy.

LB techniques were used to probe the orientation of the anionic porphyrins and their interaction with cytochrome *c*. Measurements from $\pi-A$ isotherms revealed that the porphyrin macrocycle was vertically oriented at the lipid interface, as shown in Figure 5, since the presence of the amphiphilic porphyrin **2** or **3** caused only minor perturbations of the membrane surface. The introduction of cytochrome *c* into the aqueous subphase led to binding of the protein at the lipid surface but did not cause a significant increase in the extrapolated area. Furthermore, the degree of penetration of the protein appeared to be decreased by the presence of the anionic porphyrin dopant even though the binding was much stronger (Figure 6). These observations were consistent with a surface bound cytochrome *c*, with only peripheral interactions with the lipid.

DSC techniques were employed to investigate the stability of the vesicular cytochrome *c* constructs. It was apparent that the thermodynamic characteristics of the vesicles were largely unaltered at the low concentrations of the recruiter porphyrin **4** (Figure 7). At higher porphyrin:lipid ratios, phase separation

was evident (trace c), and the presence of cytochrome *c* was found to increase the T_m and the ΔH of the putative porphyrin rich phase (trace d). Since surface lipid−protein interactions are associated with an increase in T_m and ΔH, it was inferred that the cytochrome *c* was surface bound, in concurrance with the monolayer studies. The highly cooperative transition of the porphyrin rich phase is interesting, and further research on the nature of phase separation for charged porphyrins in lipids is warranted.

That the kinetics of electron transfer within these constructs are well-behaved is instructive and worthy of comment. The change in molecularity from a first-order process in the ligated (**1**−**2**−cytochrome *c*) construct to an apparent second-order process in the unligated **1**···**3**−cytochrome *c* systems supports the formation of a defined tertiary ensemble in the former. Excluded by these data are any scenarios in which dissociation and reassociation of cytochrome *c* occur to a significant extent at the membrane surface. Any such processes would be expected to lead to the production of nonproductive complexes (e.g., Mn(III)**1**−**2**−*ferri*cytochrome *c*) over the time course of the reaction which would disturb the first-order behavior of the **1**−**2**−**Cc** (cytochrome *c*) construct. Consider the kinetic scheme in eq 1.

$$\text{Mn(II)}\mathbf{1}-\mathbf{2} + \text{Fe(III)}\mathbf{Cc} \underset{k_{-1}}{\overset{k_1}{\rightleftharpoons}} \text{Mn(II)}\mathbf{1}-\mathbf{2}-\text{Fe(III)}\mathbf{Cc} \xrightarrow[\text{et}]{k_2} \text{Mn(III)}\mathbf{1}-\mathbf{2}-\text{Fe(II)}\mathbf{Cc} \quad (1)$$

We know from the observed formation of the ternary complex **1**−**2**−cytochrome *c* that $k_1 \gg k_2$. Given that k_2 has been determined to be 1.9×10^{-3} s^{-1}, we find by kinetic simulation[25] that k_1 must be $>5 \times 10^3$ M^{-1} s^{-1} to avoid the appearance of a lag period in the time course of electron transfer corresponding to the association of cytochrome *c* with **1**−**2**. Since k_1/k_{-1} is also determined to be 5×10^6 from the UV difference titration of **2** with cytochrome *c*, k_{-1} must be at least 5×10^{-3} s^{-1}. Further, however, k_{-1} cannot be $\gg k_2$ without perturbation of the kinetics by rapid redistribution and loss of *registration* of the productive Mn(II)**1**−**2**−*ferri*cytochrome *c* complex. *Intra*-complex reorganization among several similar conformations of the interaction of **2** with cytochrome *c* and the prospect of conformational gating, which seems likely, is accommodated by the data.[26]

As we have described,[7] the rates of intracomplex electron transfer in the **1**−**2**−cytochrome *c* constructs can be compared to published data as a probe of distance. A plot of rate versus distance for five cases of electron transfer to cytochrome *c* over known distances and *at the same driving force* (∼350 mV) produces a straight line with a slope (β) of 1.2 Å^{-1} (Figure 12). As has been discussed by Rogers,[9b] reorganization energies (λ) for electron transfer into and out of heme proteins are all near 1 eV. Thus, an extrapolation of the line produced by the earlier data in Figure 12 will afford a prediction of distance for a measured electron transfer rate in the slower regime under consideration here. The data for the **1**−**2**−cytochrome *c* constructs in Table 2 indicate a Mn-heme to Fe-heme distance of 22−23 Å, *independent of the length of the intervening tether*.

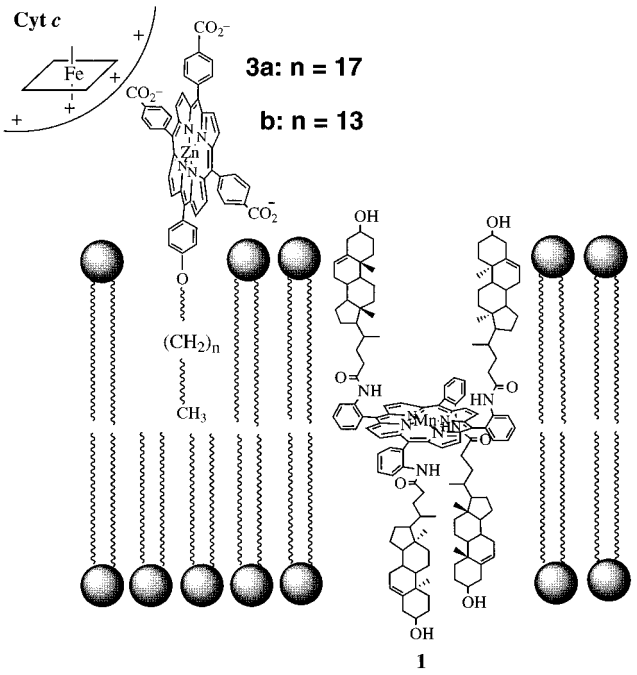

Figure 11. Cartoon of the vesicular assembly when cytochrome *c* is recruited to the membrane via anionic amphiphilic porphyrins lacking the terminal imidazole. The cytochrome *c*−**3** complex is free to laterally diffuse in the membrane, and hence, on average the heme of the protein would be further away from the Mn(II) in **1**. One might suppose however that at very large distances the electron transfer rate would be extremely slow and hence the rates reported might represent only those which occur at distances where the protein complex is not laterally displaced to a large extent.

We interpret this to mean that the cytochrome *c* is bound at the surface of the lipid for all tether lengths and that the main electron transfer pathway cannot be through the σ bond network of the tether. Rather, the electron must traverse many similar pathways which may involve the intervening lipid and the steroidal scaffolding of **1**.[27] In such a case, the lack of a terminal imidazole in the linker would not prevent electron transfer to the surface-docked cytochrome *c*. On the other hand, if the tether were the main electron transfer pathway,[28] the lack of ligation and the resulting spacial registration would decrease the efficiency of electron transfer significantly.

Figure 11 depicts the formation of two independently diffusable species, cytochrome *c*−ZnTCAmP (**3**) and MnChPCl (**1**), in the vesicle bilayer. The data are well-accommodated by a second-order fit. One can estimate a first-order rate constant of 3.8×10^{-4} s^{-1} (versus 2×10^{-3} s^{-1} in the ligated **1**−**2**−cytochrome *c* construct) from the initial rate (Figure 8) at low concentrations of Fe(II) at the onset of the reaction when [Mn(II)] ≫ [Fe(II)]. The lower value of the rate constant for **3** probably reflects a longer average distance the electron has to traverse as shown in Figure 11. However, the well-behaved kinetics of the electron transfer indicates that ligation is not a prerequisite for electron transfer.

The results obtained with the shorter lipid (DLPC) indicate that the electron transfer rate is sensitive to the width of the bilayer. The steroidal moieties are attached to the porphyrin macrocycle in **1** via flexible three-carbon linkers and, thus, could accommodate the shorter bilayer. The resultant change in the

(25) Kinetic simulations were carried out using the program HopKINSIM 1. 7. 2 on a Macintosh IIsi. For **2a**, $k_2 = 1.9 \times 10^{-3}$ s^{-1}. The simulation was based on the kinetic scheme shown in eq 1. The initial concentrations of **Mn(II)1**−**2** and Fe(III)cytochrome *c* were considered to be 3.5 μM. k_1 was varied from $k_1 = 10^9$−10^{-4} such that the ratio $k_1/k_{-1} = 5 \times 10^{-6}$ was a constant. Only when k_{-1} was ∼5k_2 did the lag time for the appearance of Fe(II)cytochrome *c* disappear.

(26) (a) McLendon, G. In *Metal Ions in Biological Systems*; Sigel, H., Sigel, A., Eds.; Marcel Dekker Inc.: New York, 1991; Vol. 27. (b) Zhou, J. S.; Kostić, N. M. *J. Am. Chem. Soc.* **1992**, *114*, 3562. (c) Zhou, J. S.; Nocek, J. M.; DeVan, M. L.; Hoffman, B. M. *Science* **1995**, *269*, 204.

(27) (a) Harriman, A.; Heitz, V.; Sauvage, J.-P. *J. Phys. Chem.* **1993**, *97*, 5940. (b) Gruschus, J. M.; Kuki, A. *J. Phys. Chem.* **1993**, *97*, 5581. (c) Evenson, J. W.; Karplus, M. *Science* **1993**, *262*, 1247.

(28) (a) Beratan, D. N.; Onuchic, J. N. *Photosynth. Res.* **1989**, *22*, 173. (b) Onuchic, J. N.; Beratan, D. N. *J. Chem. Phys.* **1990**, *92*, 722. (c) Gray, H. B.; Winkler, J. R. *Pure Appl. Chem.* **1992**, *64*, 1257.

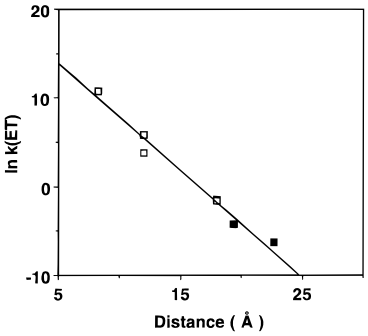

Figure 12. Electron transfer rate versus edge-to-edge distance for cytochrome *c* related systems, in the literature, having a driving force of ~0.35 eV and $\lambda \sim 1$ eV.[7] The data points (light squares) were fit to the best straight line. The darkened squares represent the rates experimentally obtained (for **2c**) versus the distance between the Mn(II) and Fe(III), for the two vesicular systems DPPC/DMPC and DLPC (see Table 1).

width of the single lipid leaflet is ~5 Å,[29] which corresponds to a decrease in the Mn to Fe distance to ~19.5 Å. From Figure 12, it can be deduced that the extrapolated distance for **2c** ($k = 1.5 \times 10^{-2}$, $\ln k = -4.19$) is ~19 Å, which is in remarkable accord with the expected value for this construct in DLPC, showing that the rate has changed in a predictable manner for the inferred structure of these assemblies.

Reduction of cytochrome *c* by Mn(II)ChP (**1**) was also observed in the absence of the recruiter porphyrin (**2** or **3**). The kinetics were second order as expected. The pseudo-first-order (initial) rate constant obtained was $\sim 10^{-4}$ s^{-1} in DMPC/DPPC vesicles which was similar to that obtained when **3** was used to recruit cytochrome *c* to the surface. However, the *efficiency* of cytochrome *c* reduction was less than half that observed with **3** under otherwise identical conditions. Thus, when ~85−90% of Mn(II) was formed during the photoreduction, there was ~60% formation of reduced cytochrome *c* when **2** or **3** was present whereas only ~25% of the expected amount of *ferro*cytochrome *c* was formed in the absence of these surface receptor molecules. The results were similar in DLPC vesicular systems.

Clearly, the recruiter zinc amphiphilic porphyrins **2** and **3** serve mainly to position the cytochrome *c* with respect to the membrane surface and, in the case of **2**, to establish the physical connection with the manganese(II) reductant (**1**), since it does not seem to affect the rate of electron transfer. The zinc porphyrin **2** also plays an important role by sensitizing the photoreduction of **1**.[30] The photoreduction was very sensitive to the extent of air-degassing, and the addition of HEPES buffer greatly increased the efficiency of the photoreduction. Typically, there was about 40−50% photoreduction of the Mn(III), but the presence of HEPES resulted in ~90% photoreduction under otherwise identical conditions. Obviously, as well, the amphiphilic zinc porphyrins **2** and **3** provided convenient spectroscopic probes with which to monitor interactions with both the cytochrome *c* and the membrane spanning porphyrin **1**, since it is the only fluorophore in the ternary assembly and has well-characterized photophysical properties. Further, the Soret maximum of **2** (and **3**) at 430 nm made it easier to visualize spectral changes, since the Fe(III)cytochrome *c* Soret maximum is at 410 nm and Mn(III) has its maximum at 476 nm. Electron transfer experiments using the porphyrin free bases **2a**−**c** also resulted in unimolecular electron transfer kinetics from Mn(II) to the ferrocytochrome *c*, at essentially identical rates. Thus, it seems unlikely that a zinc porphyrin radical anion is an intermediate in this electron transfer pathway.

This study mimics the functional role of cytochrome *c* as a peripheral membrane electron transfer protein. Model studies on cytochrome *c* recruitment to pure negatively charged lipids have shown that the protein undergoes a transition whereby the axial methionine−Fe bond is weakened, leading to an equilibrium between a 6-coordinate low-spin Fe(III) and a 5-coordinate high-spin Fe(III).[31] Such structural changes may induce weak peroxidase and/or P-450 like activity to the protein.[31b,32] However, mixtures of negatively charged and neutral lipid do not induce such major changes and enable the heme to remain 6-coordinate, precluding its ability to bind an exogenous ligand. We do not observe the UV spectral changes expected for such a transition[31a] in cytochrome *c* in these constructs, indicating that the heme remains 6-coordinate.

Conclusion

We have sought to construct complex, multicomponent membrane ensembles with both small molecule and protein components. Construction strategies have been based on the principles of molecular recognition and self-assembly. The resultant constructs have been characterized by diagnostic spectroscopic behavior and by use of LB and DSC techniques. All of the data are in accord with a surface-associated *ferri*-cytochrome *c* tethered to a manganese(II) porphyrin in the middle of the membrane bilayer. Electron transfer rates in this membrane ensemble have been measured that are consistent with a spatially well-defined system which is amenable to further photophysical investigation. We envision as well the creation of related membrane nanoassemblies which can achieve pH gradients as the result of redox behavior and, more generally, relay membrane surface recognition events for detection by membrane subphases.

Experimental Section

Materials and Methods. All water used was distilled and deionized (Millipore, Milli-Q). Phospholipids and horse heart cytochrome *c* were purchased from Sigma Chemical Co. Chromatographic separations employed silica gel (Aldrich 200−400 mesh, 60 Å). All solvents were reagent grade or HPLC grade. Thin layer chromatography was performed on Silica gel G or GF (Analtech). DMF was dried over potassium hydroxide, and methylene chloride was distilled over calcium hydride before use.

UV spectra were recorded on a Hewlett-Packard HP8452A spectrophotometer. Fluorescence spectra were acquired on a Perkin-Elmer MPF66 fluorimeter. FAB mass spectra were acquired on a Kratos MS50 mass spectrometer. ^{1}H- and ^{13}C-NMR spectra were acquired on GE QE 300 and JEOL GSX 270 spectrometers. Photochemical reduction of Mn(III)ChPCl (**1**) was accomplished using a Xenon arc

(29) The half-width of the bilayer changes by ~5 Å. Assuming an all-trans configuration the projected length of a C−C bond on the bilayer normal is 1.25 Å; hence, the change from C16(DPPC) to a C12(DLPC) lipid is 4 × 1.25 Å. The change in the bilayer width might be considered the lower limit on account of the DLPC being above the transition temperature and thus being shorter than if it were in an all-trans configuration. However, the steroidal appendages would probably restrict the degree to which the bilayer would shrink, in its vicinity. Moreover, the steroidal porphyrin reduces the extent of the gauche conformations above the transition temperature.[16b] Besides, 20% DMPC is present in the original lipid mixture, and hence the difference of four carbon atoms might be an overestimation. See: Seelig, A.; Seelig, J. *Biochemistry* **1974**, *13*, 4839.

(30) (a) Harriman, A.; Porter, G.; Richoux, M. C. *J. Chem. Soc., Faraday Trans. 2* **1981**, *77*, 833. (b) Toshiyuki, K.; Yamamura, T.; Saito, T.; Sasaki, Y. *Chem. Lett.* **1981**, 503.

(31) (a) Hildebrandt, P.; Heimburg, T.; Marsh, D. *Eur. Biophys. J.* **1990**, *18*, 193. (b) Hamachi, I.; Fujita, A.; Kunitake, T. *J. Am. Chem. Soc.* **1994**, *116*, 8811.

(32) (a) Radi, R.; Thomson, L.; Rubbo, H.; Prodanov, E. *Arch. Biochem. Biophys.* **1991**, *288*, 112. (b) Akasaka, R.; Mashino, T.; Hirobe, M. *Arch. Biochem. Biophys.* **1993**, *301*, 355.

lamp (Oriel Corp. Model 6140) fitted with 4078 Bor Crown Glass (2 in. diameter, 200 mm FL), and arc lamp power source (Oriel Model 8540).

Monolayer Experiments. The monolayer experiments were carried out in Teflon troughs either obtained from KSV Instruments (Helsinki, Finland) or custom designed in-house. All isotherms and various plots of π, mean molecular area, and time were collected on an LB5000 (KSV Instruments) system with computer controlled film balance and barrier movement, using the KSV software package for data acquisition.

Differential Scanning Calorimetry. Heat capacity measurements of the lipid and lipid−protein dispersions were performed on a MicroCal (MC2) differential scanning calorimeter at a scan rate of 20 °C/h. The data were processed using the accompanying software package. All scans were performed with phosphate buffered dispersions. An amount of buffer corresponding to the volume of the added protein solution was added to the lipid dispersions to rule out any concentration effects.

Vesicle Preparation. Vesicles containing MnChPOH (**1**) were prepared in the following manner. In a 5 mL test tube, 30 μL (500 mM) of Mn(III)ChPCl in chloroform was added to a prepared lipid aliquot (10 mmol total, 0.0053 g of L-α-dipalmitoylphosphatidylcholine (DPPC), 0.0012 g of L-α-dimyristoylphosphatidylcholine (DMPC), or 10 mmol (0.0062 g) of L-α-dilaurylphosphatidylcholine (DLPC)). Experience has shown that the DPPC/DMPC mixture afforded robust dispersions of **1**. The chloroform was evaporated under a gentle stream of argon to form a thin film and subsequently placed under vacuum for 30 min. Following the addition of 3 mL (5 mM, pH 8.0) of phosphate buffer, the mixture was sonicated using a probe tip sonicator (Branson Model 250, power level 3, titanium tip) placed to a depth of 5 mm from the solution surface. Sonication was continued until the vesicular solution appeared transparent when viewed against a black background. The vesicular solution was then centrifuged to remove titanium dust and other insoluble materials. UV analysis of the vesicular suspension indicated that ligand exchange to afford MnChPOH (**1**) had occurred during the course of these manipulations. The resultant solution was used in the electron transfer experiments described herein.

Transmission Electron Microscopy (TEM). All TEM work was done on a Philips CM 20 microscope, using carbon coated Cu grids. Glutaraldehyde (2%) and/or OsO_4 (2%) was used successively for fixing, and uranyl acetate (2%) was used for negative staining.

Molecular Modeling. Modeling studies were carried out on a Silicon Graphics Indigo 2 using the InsightII graphics program. The program was used to compute an energy grid for the cytochrome *c*, and the anionic porphyrin was manually docked to the protein. The cytochrome *c* structure was imported from the Brookhaven Protein Data Bank, using the structure of bonito heart cytochrome *c* (Kakudo, M., 1976) for modeling investigations.

Syntheses. Synthesis of MnChP (1). α,*β*,α,*β*-*meso*-[Tetra(*o*-3*β*-hydroxy-5-cholenylamidophenyl)porphyrinato]manganese(III) chloride (**1**) was synthesized as we have previously described.[5b]

Syntheses of ZnTCImP (2a−c). The syntheses of the amphiphilic porphyrins **2a**−**c** have been reported as supplementary material in the paper preceding this paper.[7]

Synthesis of *meso*-[Tris(*p*-carboxyphenyl)[4-(stearyloxy)phenyl]-porphyrinato]zinc(II) (ZnTCAmP, 3a) and *meso*-[Tris(*p*-carboxyphenyl)[4-(myristoyloxy)phenyl]porphyrinato]zinc(II) (ZnTCAmP, 3b). The characterization (^{1}H NMR and mass spectra (FAB)) for **3a** and its precursors have been reported.[8]

Synthesis of 3b. The synthesis was performed as described for **3a**[8] by the Adler type condensation of 4-carboxybenzaldehyde (13 mmol) and 4-(myristoyloxy)benzaldehyde (3 mmol) in refluxing propionic acid (40 mL). The desired 3:1 condensation product was obtained as the major product. For ease of chromatographic separation, the crude product was converted to its trimethyl ester (thionyl chloride/methanol) and the 3:1 condensation product was purified by flash column chromatography on silica gel to obtain 7% (based on 4-(myristoyloxy)-benzaldehyde) of the trimethyl ester of free base **3b**: ^{1}H NMR ($CDCl_3$, 270 MHz) δ 0.87 (t, 3 H), 1.25 (br s, 20H), 1.56 (m, 2H), 1.95 (m, 2H), 4.09 (s, 9H), 4.22 (t, 2H, J = 6.50 Hz), 7.26 (d, 2H, J = 8.6 Hz), 8.09 (d, 2H, J = 8.6 Hz), 8.27 (d, 6H, J = 7.9 Hz), 8.43 (d, 6H, J = 7.9 Hz), 8.76 (br s, 6H), 8.9 (br d, 2H); FABMS (nitrobenzyl alcohol matrix) *m*/*z* 999 (12), 1000 (74), 1001 (100), 1002 (62), 1003 (28), 1004 (9). Subsequent hydrolysis (NaOH/methanol)[7,8] yielded the free base porphyrin (H_2TCAmP) (90% yield) which was then metalated to yield **3b**. H_2TCAmP (10 mmol) was stirred in a 15 mL mixture of 1:1 chloroform−methanol containing $Zn(OAc)_2 \cdot 2H_2O$ (40 mmol). The progress of the reaction was monitored by UV spectroscopy. After the reaction was complete (∼2 h) the solvent was evaporated to dryness. The residue was then dissolved in aqueous 1% potassium hydroxide and then washed with methylene chloride to remove excess zinc acetate. The organic layer was discarded. Treatment of the aqueous layer with a few drops of glacial acetic acid resulted in the precipitation of the zinc porphyrin. The solid was collected by centrifugation and washed twice with water to give ZnTCAmP in 90% yield: vis (methanol) λ_{max} (log ϵ) 404 nm (sh), 424 nm (5.71), 558 nm (4.31), 598 nm (3.87).

Electron Transfer Experiments. In a typical experiment, a vesicular solution containing 15 nmol of **1** was transferred to a quartz cuvette equipped with a septum. To this mixture 20 μL of a 500 μM solution (1:1 methanol/water) of the zinc amphiphilic porphyrins (**2a**−**c**, **3a**,**b**) was added. The ligation (for **2a**−**c**) was allowed to proceed to completion. After ∼2 h, the contents were degassed by bubbling in a gentle stream of argon for ∼45 min to remove dissolved oxygen. Thereafter, the cuvette was exposed to Xe lamp radiation, which resulted in the photoreduction of the Mn(III). The photoreduction was monitored by the formation of Mn(II) at 444 nm, care being taken to ensure that the cuvette remained cool by intermittent irradiation for periods never exceeding 30 s. Immediately following the photoreduction, 10 μL of 1 mM cytochrome *c* (rigorously degassed) was injected through the septum. The progress of the reaction was followed by monitoring absorbance changes being tabulated every 12 s for DMPC/DPPC vesicles (every 5 s for DLPC vesicles), at 410 nm [Fe(III)-cytochrome *c*], 430 nm [Zn in **2** and **3**], 444 nm [Mn(II) in **1**], 476 nm [Mn(III) in **1**], 550 nm [Fe(II) cytochrome *c*], and 790 nm [background]. The measurements were made automatically in the kinetic scanning mode of the diode array UV spectrometer, and reactions were followed for 1200 s. To obtain absorbances at time $t = \infty$, a UV spectrum was recorded after ∼1 h, and small changes were made in the values obtained to get the best fit for the kinetic data. Rate constants were obtained from these data by standard kinetic fitting routines.

Acknowledgment. Support of this research by the National Institutes of Health (Grant GM 36928) is gratefully acknowledged. We thank Dr. Mark Witmer from Bristol-Myers Squibb for help with the DSC and Dr. Eric P. Kelson for help with the cyclic voltammetry.

JA953092E